



Comparison between LoRa and NB-IoT coverage in urban and rural Southern Brazil regions

Lucas Eduardo Ribeiro¹ · Davi Wei Tokikawa¹ · João Luiz Rebelatto¹ · Glauber Brante¹

Received: 8 November 2019 / Accepted: 1 June 2020 / Published online: 30 July 2020
© Institut Mines-Télécom and Springer Nature Switzerland AG 2020

Abstract

In this work, we resort to computer simulations to compare the coverage of long range (LoRa) and narrowband (NB)-IoT in two different realistic scenarios of southern Brazil, encompassing an overall area of 8182.6 km². The first scenario is predominantly rural with a few base stations (BSs) while the other scenario corresponds to a mostly urban area with high density of BSs. Our analysis, which adopts the actual position and parameters of the BSs of a given operator, also takes into account the digital elevation model (DEM) of the environments in order to calculate the path loss, following a realistic propagation model from 3GPP. Our results indicate that for a mainly rural environment, when operating at a similar sub-GHz frequency band, NB-IoT outperforms LoRa due to the directivity associate with directional antennas which provide a better coverage for devices which are far from BS but near the main beam. However, LoRa presents a better coverage, regardless of the site deployment, when the NB-IoT is considered to operate in the 1900-MHz band.

Keywords Coverage · LoRa · NB-IoT · IoT

1 Introduction

Over the last years the prospects to the Internet of Things (IoT) market have been growing in quantity as well as in number of applications [1, 2]. Due to the demand imposed by this market, new wireless technologies are emerging in order to enable power efficient wireless communication over very long distances [3]. Such long-range wireless technologies deployed for the IoT usage can be divided into

two main categories: Cellular and Low-Power Wide-Area Networks (LPWAN). The cellular networks, which have been so far represented mainly by General Packet Radio Service (GPRS), have currently the Narrowband (NB)-IoT as its frontrunner technology [4, 5]. Standardized by 3GPP (3rd Generation Partnership Project), NB-IoT aims at supporting a massive number of low-throughput devices, with low cost and improved power efficiency [6]. Regarding LPWAN, the long range (LoRa) technology is certainly one of the main representative technologies in this category [7]. It uses a proprietary spread spectrum modulation scheme that enables the signal to reach long distances, while transmitting with low data rate and low power [8], and usually relying on the LoRaWAN architecture to define the higher layers.

A coverage analysis for NB-IoT is addressed in [9], where simulation results indicate that improvements on Maximum Coupling Loss (MCL) in the order of 20 dB can be achieved over traditional Long-Term Evolution (LTE) technology. In [10], the authors discuss issues related to the deployment of NB-IoT only in a subset of base stations (BSs), for example the upgrade of just some BSs with NB-IoT within a region: this arrangement can cause strong co-channel interference from the non NB-IoT cells. As shown in [10], this problem can be avoided by jumping the Physical Resource Block (PRB) used by LTE-only BSs,

This work has been partially supported by CNPq and CAPES (Brazil).

✉ Lucas Eduardo Ribeiro
lucaseduardor@hotmail.com

Davi Wei Tokikawa
tokikawa@alunos.utfpr.edu.br

João Luiz Rebelatto
jlrebelatto@utfpr.edu.br

Glauber Brante
gbrante@utfpr.edu.br

¹ CPGEI, Universidade Tecnológica Federal do Paraná, Curitiba, PR, Brazil

i.e., BSs without NB-IoT deployment should leave the PRB destined for NB-IoT unused.

The coverage of LoRa is studied in [11], where a proprietary software was used to estimate the LoRa coverage for two cities in Argentina, whose result is supported by actual measurements. In [12], Hoeller et al. proposed a theoretical model to derive coverage probability which includes both internal interference, due to imperfect Spreading Factor (SF) orthogonality, and cross-technology interference.

A more detailed and wider coverage comparison is presented in [13], where LoRa, Sigfox [14], GPRS, and NB-IoT technologies are compared in a region of northern Denmark. The purpose of the authors was to evaluate the performance of these technologies for outdoor and indoor-located devices, considering realistic rural and urban environments. Moreover, in order to get more realistic results, a Digital Elevation Model (DEM) of the environment, along with the information of areas with valid household numbers, was taken into account. It was shown that NB-IoT provides better coverage among all the aforementioned technologies, for both rural and urban scenarios. An analysis performed in [15], extending the work done in [13], showed that even when considering the probability of collisions and blocking, NB-IoT outperforms the other technologies. A similar study involving coverage and capacity for rural areas was developed in [16], in which the authors compare two User Equipment (UE) categories proposed by 3GPP: NB-IoT and LTE-M. The results showed that despite NB-IoT providing better coverage, LTE-M supports more devices thanks to its lower overhead and larger bandwidth.

In this paper, we compare LoRa¹ and NB-IoT in terms of coverage in two different realistic scenarios of southern Brazil, encompassing an overall area of 8182.6 km². Differently from [13], our analysis encompasses all the considered area when evaluating a given technology coverage, and not only the portions of the selected region with a household number, i.e., with valid addresses. Therefore, our analysis is focused on outdoor scenarios, while indoor communication has been considered by [13]. The aim is to compare different BS densities for the two proposed technologies, as well as to evaluate the effects of NB-IoT operating at stand-alone mode under two bands, namely 850 and 1900 MHz, that are currently available to GPRS technology in the regions taken into account [17].

In our analysis, we adopt the 3GPP path loss model [18], which can account for both rural and urban scenarios. In addition, a two-dimensional correlated shadowing model

¹Note that, even though LoRa refers only to the Physical (PHY) Layer, the term NB-IoT encompasses a complete PHY, Multiple Access (MAC), and Network solution. However, since our aim is to compare coverage, which depends basically on PHY parameters, we opted for keeping the nomenclature LoRa instead of the more complete LoRaWAN, as in [13].

is employed, following [19], while we also consider the DEM of the regions under study, obtained from the TOPODATA database, provided by the Brazilian National Institute of Research (INPE) [20]. Finally, we consider the site deployment (BS positioning, antenna heights, etc.) of a given network operator for the NB-IoT, and also suppose that the LoRa BSs are placed in the same positions of the NB-IoT BSs, for fair comparison purposes. Our results indicate that NB-IoT and LoRa technologies can have more than 90% coverage in both urban and rural outdoor scenarios. Furthermore, similar to [13], we also show that NB-IoT provides wider coverage than LoRa operating in a sub-GHz band with low density of BSs. However, LoRa showed to be more advantageous than NB-IoT when the density of BSs is higher and when NB-IoT operates in the 1900-MHz band.

The rest of this paper is organized as follows. Section 2 briefly compares the two aforementioned technologies and present the assumptions used in the simulations. Section 3 presents the simulation model and the regions under analysis. Then, Section 4 provides simulation results and their analysis. Finally, Section 5 concludes the paper.

2 Preliminaries

2.1 LoRa versus NB-IoT

2.1.1 LoRa

LoRa [8] is a proprietary spread-spectrum modulation scheme patented by Semtech, which trades between data rate and sensitivity, enabling long range, low data rate, and low power communications [6]. A LoRa device can be configured to use different parameter settings such as transmission powers, bandwidth settings (BW), coding rates (CR), and spreading factors (SF), resulting in different trade-offs [24]. To increase receiver sensitivity and achieve higher coverage ranges, one can vary SF from 7 to 12, where higher SFs mean higher communication range at the cost of lower data rate [25].

Spreading the transmitted signal into a larger bandwidth makes it more resistant against interference, which allows the signal to be decoded even when the signal power is several times below the noise floor [1]. To evaluate the cross-technology interference, the authors in [26] set up an experiment to measure the interference of IEEE 802.15.4g technology in LoRa networks: they showed that LoRa can obtain high packet reception rates, even in the presence of strong IEEE 802.15.4g interference. Therefore, in our work, we follow [13] and assume that interference is negligible.

In 2015, an alliance, called LoRa Alliance [27], launched the first version of a protocol (LoRaWAN protocol)

adopting LoRa at the Physical Layer, operating in the ISM sub-GHz spectrum. LoRaWAN uses ALOHA scheme at MAC Layer and has a network architecture deployed in a star-of-stars, where devices do not connect to a LoRaWAN gateway/BSs, instead the BS forwards every message received from LoRaWAN devices in range, thus exploiting redundancy of messages at different BSs [1, 6].

Since we are interested on evaluate coverage, in practice, we push these parameters to its bounds (SF = 12, BW = 125 kHz, and transmit power = 20 dBm), such that they represent the most robust setup with respect to coverage, i.e., MCL = − 157 dB [21, 28]. Besides, it is considered that LoRa BSs use omni-directional antennas with 10 dBi gain while LoRa UEs deploy 0 dBi antennas.

2.1.2 NB-IoT

NB-IoT was proposed by 3GPP in 2016 as part of Release 13 [29], aiming at improving coverage, power efficiency, and reducing the complexity for cellular IoT devices, targeting low-throughput devices with low cost [30]. It can be deployed in a stand-alone mode (with dedicated spectrum, i.e., a channel of GSM band), in an in-band mode (within the band of a LTE carrier), or in a guard-band mode (occupying the guard band of a LTE carrier) [31, 32]. Regarding its physical layer, the highest modulation enabled is QPSK and the bandwidth is fixed at 180 kHz [6, 33], and the maximum transmitted power is 23 dBm for uplink and 43 dBm for downlink [22].

In Brazil, there are currently four GSM bands available (namely 850, 900, 1800, and 1900 MHz), which are potential candidates for NB-IoT deployments [34]. Here, we will evaluate the performance of NB-IoT when operating at the extreme values of 850 and 1900 MHz, while LoRa operates in Brazil at the ISM band of 915 MHz.

Another difference between the technologies is the antenna radiation pattern: while LoRa uses omni-directional antennas, NB-IoT adopts directional antennas at the BSs. Assuming an update of the current GSM technology deployed to NB-IoT, the direction and gains for the antennas were taken from the actual site deployment, which can be obtained from [23]. For simplicity, it was assumed that all directional antennas follow the same radiation pattern, of an antenna that is common to both sites, which was taken directly from the manufacturer's website [35]. One should also note that NB-IoT should not suffer from cross-technology interference, as it operates in a licensed band. The main characteristics of NB-IoT and LoRa are summarized in Table 1, in accordance to [21, 22].

Remark 1 As uplink and downlink for NB-IoT are not symmetrical [22, 36], the uplink channel will be employed in the simulations, since it is the most critical link for a

Table 1 Main parameters of LoRa and NB-IoT

Parameter	LoRa [21]	NB-IoT [22]
Transmit Power	20 dBm	23 dBm
MCL	− 157 dB	− 164 dB
Carrier frequency	915 MHz	850/1900 MHz
Antenna pattern	Omnidirectional	Directional
Antenna gain	10 dBi	14.67 dB ^a

^aAverage value. The exact value per antenna is obtained from the actual site deployment [23]

coverage analysis; i.e., we consider that a device is covered if the uplink loss is below the MCL for a given technology.

Remark 2 We assumed that NB-IoT devices can perfectly cope with handovers and choose the BS with the highest link budget.

2.2 Path loss

The path loss is an intrinsic characteristic of the wireless channels, caused by the power dissipation through the propagation environment [37]. Moreover, an additional attenuation is imposed due to the presence of obstacles between the transmitter and receiver, which is referred to as shadowing, and occurs mainly due to the absorption, reflection, scattering, and diffraction effects [37].

In this work we adopt the Rural and Urban Non Line-of-Sight (NLOS) path loss model proposed by 3GPP in [18], which considers both theoretical and empirical results to create an accurate model. According to [18], the path loss at a given separation distance d (in meters) between transmitter and receiver is obtained as:

$$\begin{aligned}
 PL(\text{dB}) = & 161.04 - 7.1 \log(W) + 7.5 \log(h) \\
 & - \left(24.37 - 3.7 (h/h_{\text{BS}})^2\right) \log(h_{\text{BS}}) \\
 & + (43.42 - 3.1 \log(h_{\text{BS}})) (\log(d) - 3) \\
 & + 20 \log(f_c) - \left(3.2 (\log(11.75h_{\text{UE}}))^2 - 4.97\right) \\
 & + X, \tag{1}
 \end{aligned}$$

where f_c represents the carrier frequency (in GHz), h_{UE} and h_{BS} represent respectively the heights of UEs and the BSs, while h stands for the average height of the buildings between the BS and the UE. W represents the street width and X stands for the shadowing, which is modeled as a Gaussian-distributed random variable with zero mean and standard deviation σ . In (1), all the distances are in meters and the logarithm is base 10.

As suggested in [18], the parameters in (1) have different typical values depending on the environment characteristics, as presented in Table 2. It is worthy mentioning that h_{BS}

Table 2 Typical path loss parameters [18]

Parameter	Urban macro	Rural macro
UE's height (h_{UE})		1.5 m
Street width (W)		20 m
Height of buildings (h)	20 m	5 m
Std dev. shadowing (σ)	6	8

is obtained according to the actual values of the BSs considered in the analysis, as will be explained in details later.

2.2.1 Shadowing correlation

In practice, *shadowing* in (1) for devices in close vicinity is not completely independent, presenting a certain degree of correlation. In [19], the authors present a two-dimensional shadowing model that takes into account a parameter called *correlation distance*. This model acts as a filter for the random variable that describes the shadowing, presenting uncorrelated results when the separation distance between two points is larger than the correlation distance.

Figure 1 illustrates the effect of correlation by plotting the values of a random variable before (Fig. 1a) and after (Fig. 1b) applying the proposed filter with correlation distance set to 120 m, which according to [18] is suitable for a rural environment. Moreover, each pixel on the grid

corresponds to an area of approximately $93 \text{ m} \times 93 \text{ m}$, which is the same map resolution used for the selected regions. It can be seen that the shadowing in Fig. 1a is sparse, while in Fig. 1b it is concentrated in a few spots, as indicated by the blue dots.

2.3 The regions and their characteristics

In this work, two regions with different BS densities are chosen: *Region 1* consists of a group of small cities (Castro, Carambéi, Tibagi, and Piraí do Sul) that have one of the largest dairy herd of Brazil. This region has been chosen due to its agribusiness importance and due to the fact that it has a low concentration of base stations per square kilometer (15 BSs in a overall area of 7560.6 km^2 , i.e., in average one BS every 504 km^2), being mostly composed of rural areas, as illustrated in Fig. 2a.

Next, *Region 2* comprehends, mostly, the urban area of Cascavel City, containing 32 BSs in an area of 622 km^2 , yielding one BS per 19.4 km^2 , as shown in Fig. 2b. The BS positions and characteristics (such as height, number of antennas, and coordinates) are obtained from the National Telecommunications Agency (Anatel) [23], representing the actual site deployment from a given operator.

It was assumed that devices may be anywhere in the selected region, which means that each pixel is a candidate to have an UE. Thus, the coverage analysis considers the existence of an UE in every pixel. Besides, it was also taken into account that devices could be located indoor and experience additional losses, which was simulated

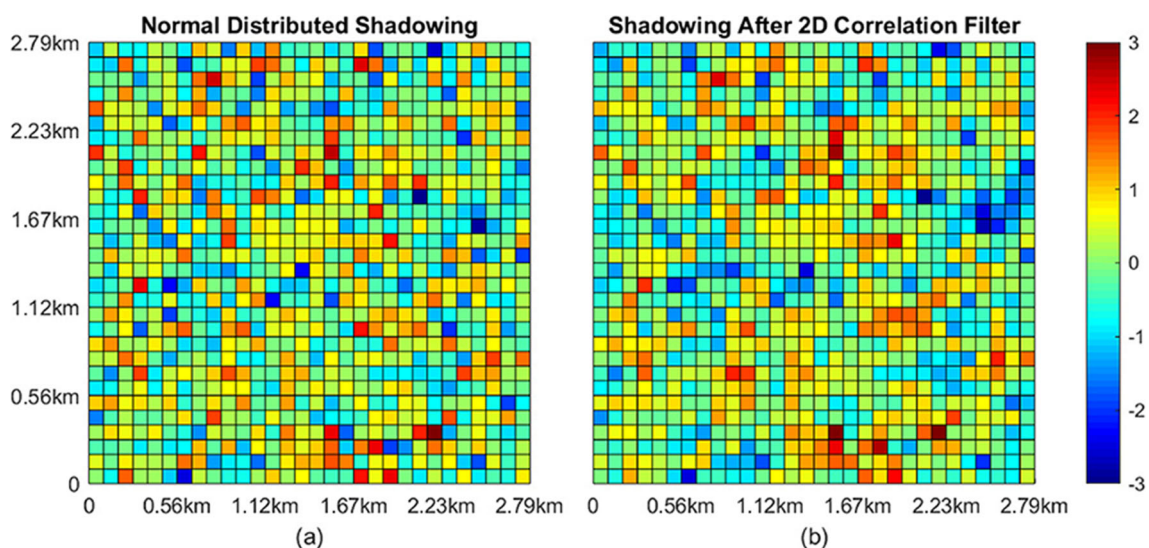


Fig. 1 Comparison between (a) uncorrelated shadowing and (b) shadowing with correlation distance of 120 m. Each pixel on the grid corresponds to an area of $93 \text{ m} \times 93 \text{ m}$. The bluer the pixel color, the greater the shadowing losses in that location; in this example with

standard deviation equals to 1, it tends toward 3 dB. On the contrary, the redder the pixel color, the smaller the shadowing losses, tending toward -3 dB

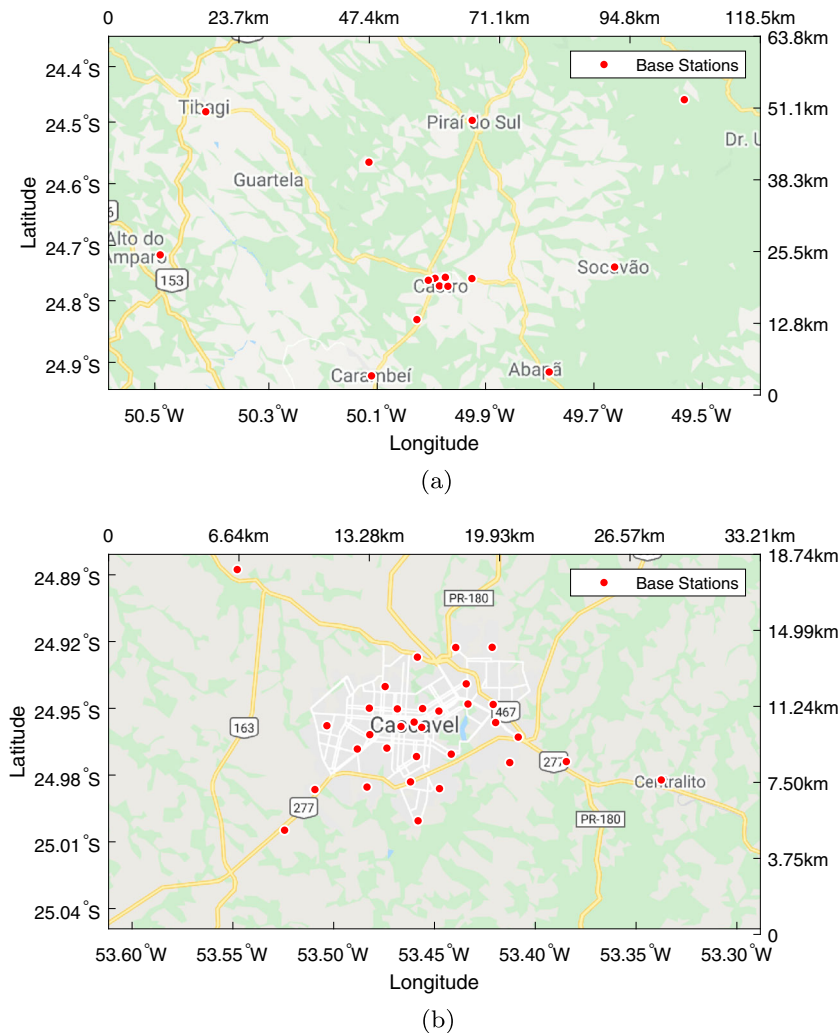


Fig. 2 Regions under study: (a) shows region 1 which is mainly rural and has 15 BSs distributed in 7560.6 km²; (b) presents region 2 which is a mostly urban area with 32 BSs distributed in 622 km²

by adding a 20 dB penalty loss to the outdoor path loss calculation.²

3 Simulation model

The algorithm developed in this work was implemented using Matlab. The block diagram presented in Fig. 3 illustrates the coverage simulation performed, which can be briefly explained as follows:

3.1 Input data pre-analysis

In this pre-simulation step, the “Detach Area” block receives the terrain data from the DEM (latitude, longitude,

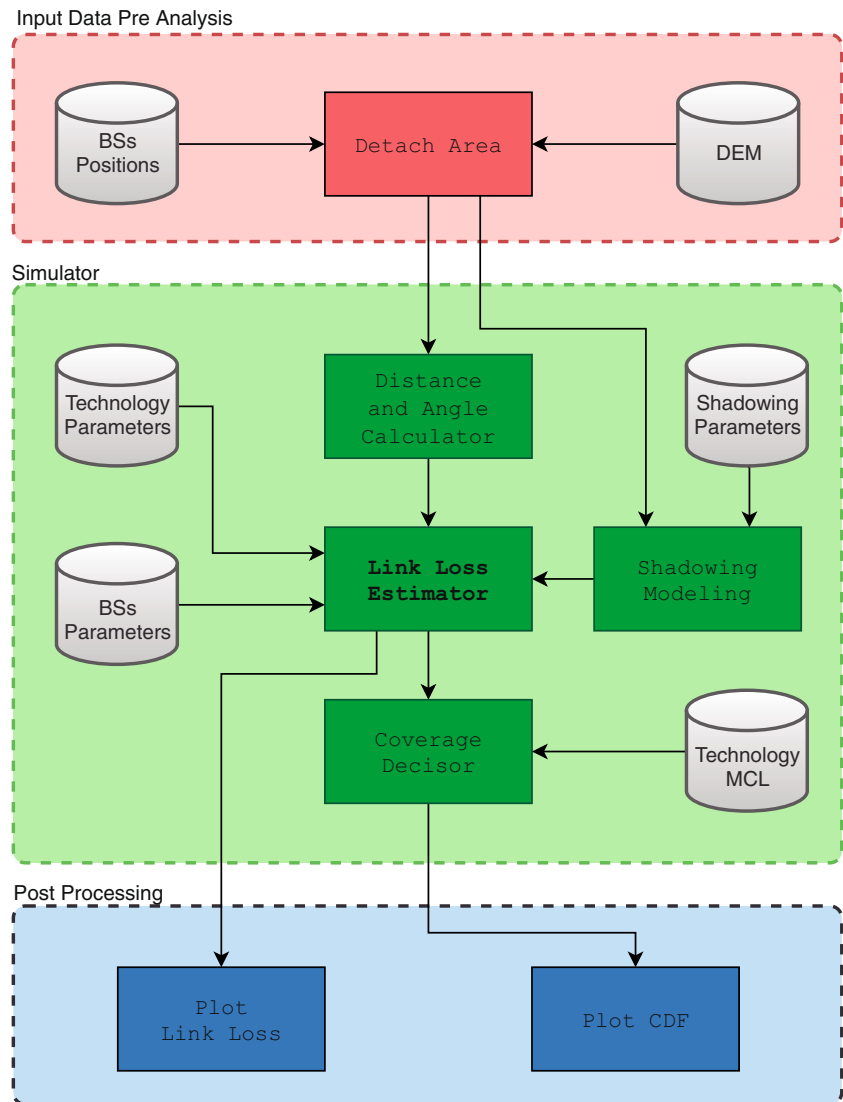
and elevation) [20], along with the coordinates data of the BSs (latitude, longitude, and height) [23]. Both data are then mixed into a single grid with resolution no smaller than 93 m × 93 m (the resolution provided by the DEM in [20]), and the area under interest is detached from the overall area in order to avoid simulations with prohibitively high time consumption. As a result, one has a grid with N_p pixels, where each pixel has a latitude, longitude, and elevation, such that there exists N_{BS} out of the overall N_p pixels with a BS, whose individual heights are in accordance to [23].

3.2 Simulation

In this step, the topology data generated in the previous stage is used to create the shadowing pattern and to calculate the angles and distances between each pixel and each BS. Then, the “Link Loss Estimator” block calculates the overall losses for each link between the BSs and the

²Note that, since we do not have the data regarding the valid addresses in the considered regions, the results when applying such additional losses can be viewed as a worst case, where all the pixels in the grid are provided with a valid address.

Fig. 3 Block diagram illustrating the proposed simulation model. The simulation was divided into three main sections. In the first section (Input Data Pre Analysis), regional parameters are loaded and undesirable areas and BSs are withdrawn. In the following, the topology parameters along with the antenna’s radiation pattern, shadowing, and technology parameters are taken as input by the “Link Loss Estimator” module, so average losses can be estimated. After estimating the overall losses, the coverage for each pixel is determined comparing MCL with link loss. Finally, in the Post Processing section, link loss and CDF graphs are generated and plotted



pixels, which, after being compared with the corresponding MCL, determines the coverage. More specifically:

- “Distance and Angle Calculator”: This block is responsible for calculating the distance and the angle from the p th pixel to the i th BS, $\forall p \in \{1, \dots, N_p\}$, $i \in \{1, \dots, N_{BS}\}$. The distance between each pixel and BS is calculated by doing the Haversine distance followed by a Pythagorean distance, which takes into account the earth’s curvature and the heights from devices and BSs. We recall that while the heights of UE devices were stipulated to be 1.5 m, the heights used for the BSs antennas were also taken from ANATEL database, which corresponds to the actual site deployment.
- “Shadowing Modelling”: Takes as input the data coming from “Detach Area” block along with correlation distance and standard deviation, delivering a shadowing grid to be used for link loss estimation.
- “Link Loss Estimator”: This block takes distances, angles, and shadowing delivered by the previous process and along with technology and BS parameters, like carrier frequency and antenna gain, to compute the overall losses.
- “Coverage Decisor”: Once the losses are calculated, this module compares the minimum loss (between the pixel and the BSs) with the MCL of the technology to be tested, to decide whether the pixel is covered or not.

Let $p \in \{1, \dots, N_p\}$ be the index of the p th pixel among the total number of N_p pixels presented in the area under consideration, and $i \in \{1, \dots, N_{BS}\}$ represents the i th BS from the total number of N_{BS} base stations. Let us also define an indicator variable $\phi^t(p) \in \{0, 1\}$ in order to indicate whether the p th pixel is covered by technology $t \in \{\text{LoRa}, \text{NB-IoT}\}$ or not, such that $\phi^t(p) = 1$ (resp. $\phi^t(p) = 0$) indicates

Table 3 Simulation parameters

Parameter	Region 1 (rural)	Region 2 (urban)
Area	7,560.6 km ²	622 km ²
N_p	880,542	72,877
BS density	504 km ² /BS	19.4 km ² /BS
Correlation distance	120 m	50 m
Map resolution	93 m × 93 m	
Terrain map	TOPODATA DEM [20]	
Path loss	Rural macro (NLOS)	Urban macro (NLOS)

that pixel p is covered (resp. not covered) by technology τ . Thus, we have that

$$\phi^\tau(p) = \begin{cases} 1, & \text{if } \min_i \text{LinkLoss}^\tau(i, p) < \text{MCL}^\tau; \\ 0, & \text{otherwise,} \end{cases} \quad (2)$$

where MCL^τ represents the maximum coupling loss of technology τ as presented in Table 1, while $\text{LinkLoss}^\tau(i, p)$ stands for the estimated overall losses of the UE placed in pixel p regarding BS i , calculated as

$$\text{LinkLoss}^\tau(i, p) = PL^\tau(i, p) + L^\tau(i) - AG^\tau(i, p), \quad (3)$$

where $PL^\tau(i, p)$ is the path loss from BS i to pixel p obtained from (1), $AG^\tau(i, p)$ is the antenna gain³ from BS i to pixel p , and $L^\tau(i)$ represents additional losses, such as those referring to indoor attenuation and cable losses (when suitable). The coverage ratio of a given technology τ is then obtained as

$$\text{CoverageRatio}^\tau = \frac{\sum_{p=1}^{N_p} \phi^\tau(p)}{N_p}. \quad (4)$$

3.3 Post-processing

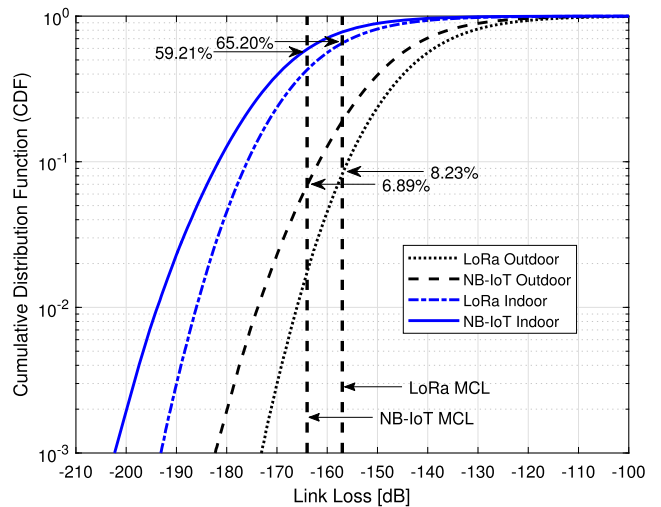
In the post-processing step, two tasks are performed independently. First, the link loss for all pixels is plotted, which allows a visual analysis about areas lacking coverage.

³Note that the antenna gain varies with different pixels in NB-IoT, due to directionality. For NB-IoT, it must also be included the transmitter antenna gain, since output transmitted power is not considered Equivalent Isotropically Radiated Power (ERPI) [22].

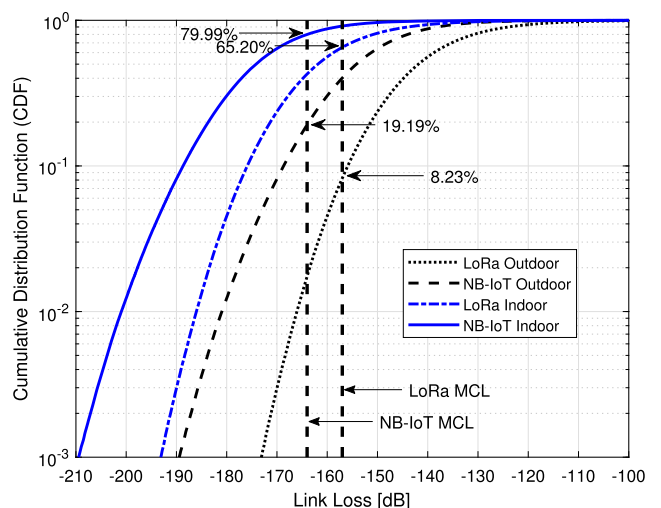
Then, the cumulative density function (CDF) for each scenario is computed and plotted.

Table 3 summarizes these simulation assumptions.

Remark 3 According to [21], the MCL for LoRa is 157 dB, while for NB-IoT the minimum MCL is 164 dB [22]. Despite this clear advantage in sensitivity, there is a conceptual difference on the transmitted power. While LoRa considers transmitted power as EIRP which already includes cable losses and transmitter antenna gains [13] [38]; for NB-IoT, such parameters must be included when calculating the link budget [22].



(a) Region 1 - LoRa and NB-IoT (at 850 MHz)



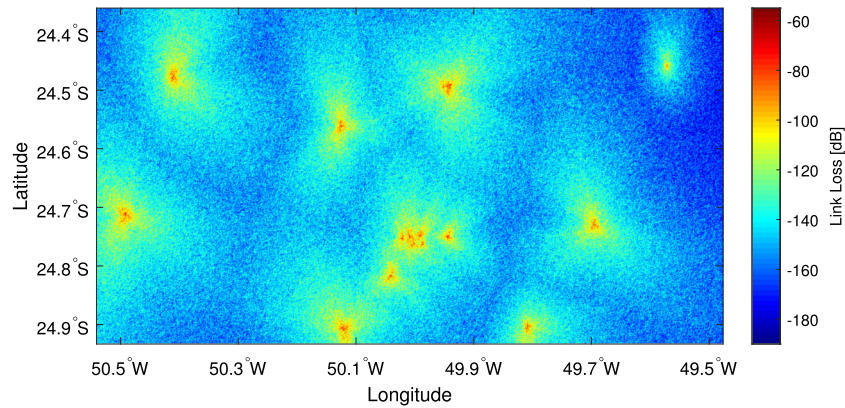
(b) Region 1 - LoRa and NB-IoT (at 1900 MHz)

Fig. 4 Cumulative Density Function (CDF) of MCL for devices in Region 1 **a** NB-IoT at 850 MHz; **b** NB-IoT at 1900 MHz

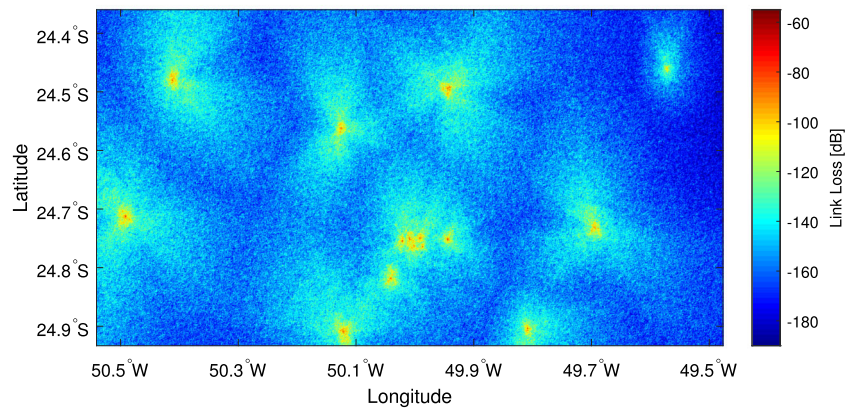
4 Results

In what follows, we present the coverage comparison between LoRa and NB-IoT following the simulation model and parameters presented in the previous sections.

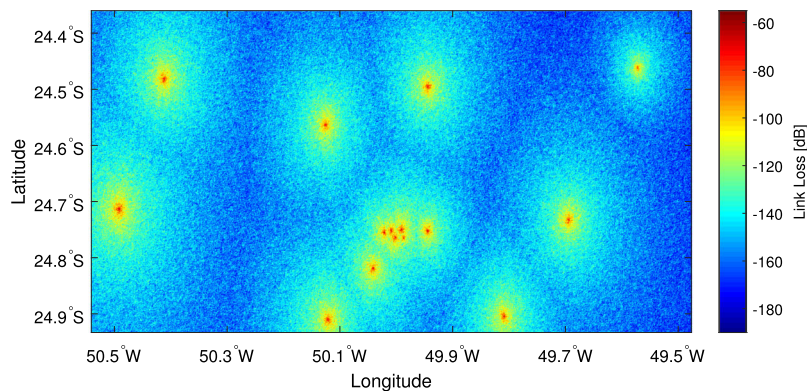
The first set of results is obtained considering Region 1, a rural area with low density of BSs, as presented in Table 3. Figure 4 represents the CDF of the Link Loss for LoRa and NB-IoT, the latter operating at both 850 and 1900-MHz carrier frequencies. The vertical dashed lines represent the



(a) Region 1 - NB-IoT (at 850 MHz)



(b) Region 1 - NB-IoT (at 1900 MHz)



(c) Region 1 - LoRa

Fig. 5 Link loss, Region 1. **a** NB-IoT at 850 MHz; **b** NB-IoT at 1900 MHz; **c** LoRa. The bluer, the greater the loss

LoRa and NB-IoT MCL as from Table 1, such that the part to the left of such threshold MCL represents the ratio of pixels in outage (not covered by the technology). As stated in Section 2.3, we also consider the additional attenuation of 20 dB to represent indoor located UEs.

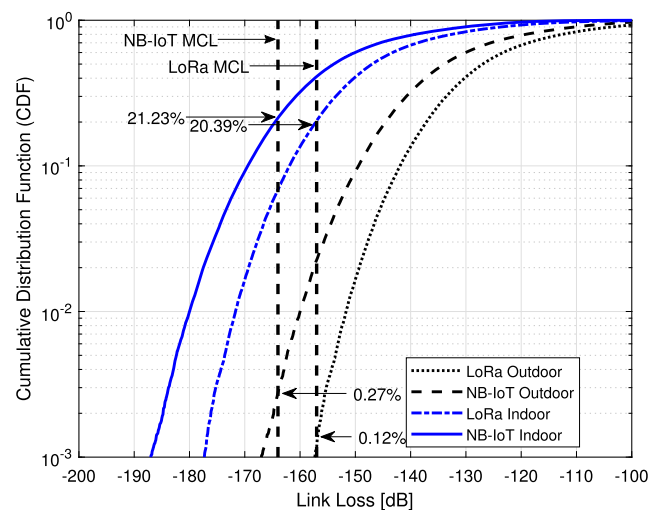
In Fig. 4, it can be seen that, when considering outdoor devices, the percentage of pixels covered was about 91.77% for LoRa users and 93.11% for NB-IoT at 850 MHz, indicating an advantage for NB-IoT, when both technologies are operating at a similar carrier frequency. However, when the NB-IoT operation band is increased to 1900 MHz, its average coverage decreases to 80.81%; this happens because the higher carrier frequency leads to a higher path loss.

As expected, the coverage decreases when indoor attenuation is also taken into account, but the comparative results remain unchanged. For indoor devices, as exposed in Fig. 4b, the percentage of covered areas decreases to 34.80% for LoRa and 40.79% for NB-IoT at 850 MHz, reaching only 20.01% of coverage when NB-IoT is operating at 1900 MHz.

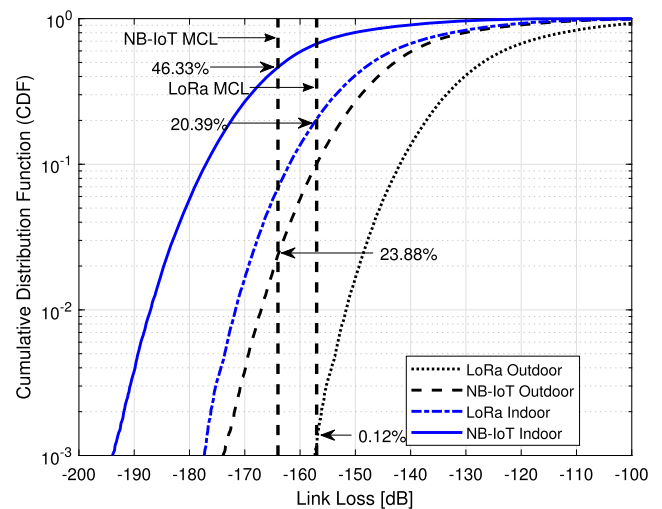
Figure 5 visually illustrates the coverage under Region 1 for outdoor users, by presenting the Link Loss between each pixel and the BS that provides the best link budget. The bluer the pixel color, the greater the loss and consequently the greater the possibility of not being covered. The opposite is also true: the more red the pixel, the lower the losses. In order to ease the visualization of Figs. 5 and 7, the link loss of LoRa is plotted with less 7 dB, which corresponds to the difference between the MCL threshold for LoRa and NB-IoT.

From Fig. 5, it can also be seen that directional antennas provide better link budget than omni-directional antennas for devices that are far away from the BSs (in the direction of the main lobe), therefore improving coverage for this set of devices. This effect is particularly relevant when analyzing rural environments, where UEs are usually far from BSs. On the other hand, for urban environments, most devices are near a BS and most of them are already covered; hence, increasing link budget in one direction does not improve the coverage rate.

Figures 6 and 7 present the same results as Figs. 4 and 5, but now considering Region 2, with a higher density of BSs. We can see in Fig. 6a that, due to the higher BS concentration, the amount of pixels not served by both technologies is smaller than 1% for outdoor devices. For indoor devices, due to 20 dB additional attenuation, the percentage of covered areas decreases to 79.61% for LoRa and 78.77% for NB-IoT at 850 MHz. Even for NB-IoT operating at 1900 MHz (the worst configuration among the three candidates), it still reaches 53.67% of coverage. These results show that for Region 2 LoRa has a slightly better



(a) Region 2 - LoRa and NB-IoT (at 850 MHz)

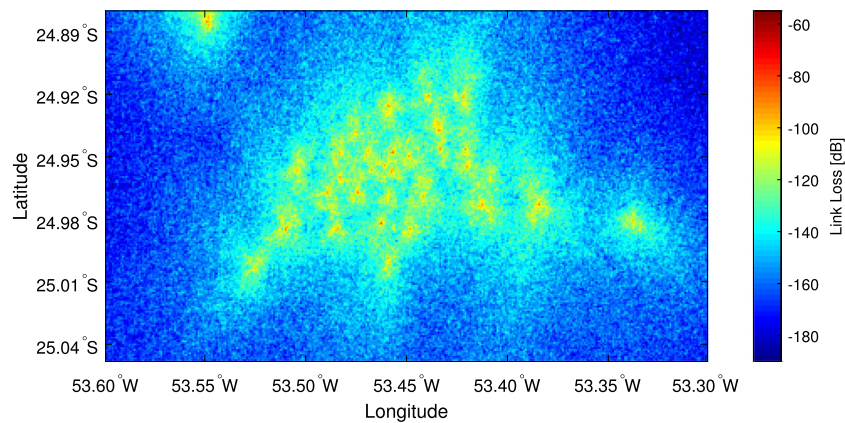


(b) Region 2 - LoRa and NB-IoT (at 1900 MHz)

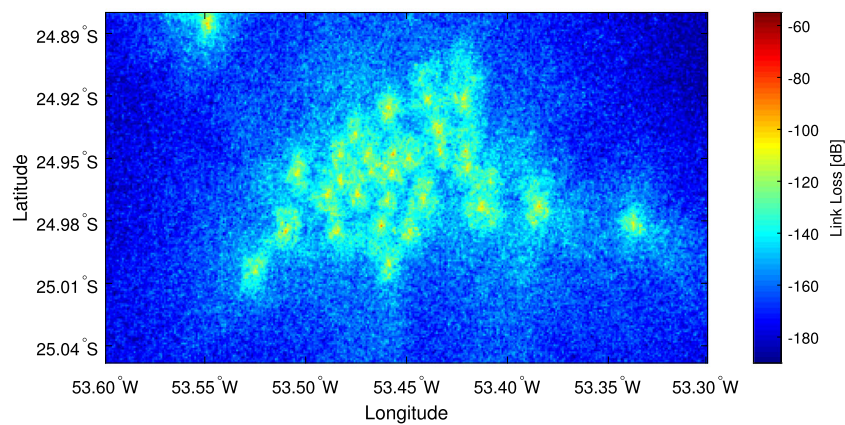
Fig. 6 Cumulative Density Function (CDF) of MCL for devices in Region 2 **a** NB-IoT at 850 MHz; **b** NB-IoT at 1900 MHz

coverage ratio, which is justified by the better performance of omni-directional antennas in serving UEs apart from the main beam direction of directional antennas.

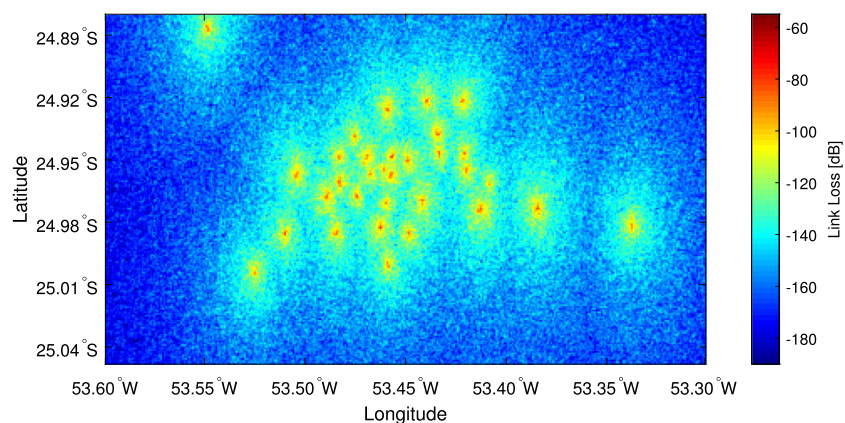
The graphs in Fig. 7 reveal where the areas with bad coverage in Region 2 are located, by considering an indoor scenario. As stated, this does not change the panorama, since indoor scenarios are simulated by just adding 20 dB over outdoor scenarios. Thanks to the characteristic of omni-directional antennas in providing equal power for azimuthal directions around the BS, for the urban scenario where all devices are closer to the BS, the advantage of directional antennas becomes unimportant and LoRa presents a slightly better coverage rate.



(a) Region 2 - NB-IoT (at 850 MHz)



(b) Region 2 - NB-IoT (at 1900 MHz)



(c) Region 2 - LoRa

Fig. 7 Link loss, Region 2. **a** NB-IoT at 850 MHz; **b** NB-IoT at 1900 MHz; **c** LoRa. The bluer, the greater the loss

5 Conclusion

In this paper, an extension of the simulation work introduced in [13] for regions in Brazil was proposed. The aim was to adapt the simulation to the site deployment of a

local network operator, at the frequency bands allowed in Brazil and to evaluate the influence of site deployment on coverage. Therefore, two regions were chosen: one mainly rural, with low BS density; and one mainly urban, with high BS density.

In the area with low BS density, the coverage for indoor devices achieves at maximum 40.79% of the pixels when using NB-IoT at 850 MHz, 34.80% when using LoRa, and less than 20.01% of pixels are served by NB-IoT at 1900 MHz, revealing a very poor coverage for indoor devices. However, excluding the scenario in which NB-IoT operates at 1900 MHz, outdoor users for this region experience a coverage of above 91.77%. Regarding the area with high BS density, coverage reaches above 97.61% for outdoor users in all scenarios. Adding 20 dB in losses to simulate indoor attenuation reduces coverage ratio to about 79.61% for LoRa, 78.77% for NB-IoT at 850 MHz, and 53.67% for NB-IoT at 1900 MHz.

One aspect that might affect the results is that we assumed that NB-IoT devices can perfectly tackle handovers and choose the BS with the highest link budget, which could be an extra source of damage for NB-IoT coverage. On the other hand, if we consider that LoRa devices are operating with LoRaWAN, there is no handover and all messages are sent to the network server, which is in charge, among other things, to handle repeated messages.

The results show that for NB-IoT operating at 850-MHz band, it provides the best coverage for a region with low BS density, but when the scenario is changed to a mainly urban with high BS density, LoRa provides slightly better coverage. These outcomes can be attributed to the fact that NB-IoT uses a directional antenna which indeed provides a better coverage near the main bearing, especially when comparing devices away from the BS, but leaves behind coverage in side lobes. Thus, we conclude that site deployment does have influence when choosing a technology based on coverage.

References

- Raza U, Kulkarni P, Sooriyabandara M (2017) Low power wide area networks: an overview. *IEEE Commun Surv Tutor* 19(2):855–873. <https://doi.org/10.1109/COMST.2017.2652320>
- Sundmaeker H, Guillemin P, Friess P, Woelfflé S (2010) Vision and challenges for realizing the Internet of Things. Publications office of the European Union, cluster of European research projects on the Internet of Things
- Al-Fuqaha A, Guizani M, Mohammadi M, Aledhari M, Ayyash M (2015) Internet of Things: a survey on enabling technologies, protocols, and applications. *IEEE Commun Surv Tutor* 17(4):2347–2376. <https://doi.org/10.1109/COMST.2015.2444095>
- Mekki K, Bajic E, Chaxel F, Meyer F (2019) A comparative study of lpwan technologies for large-scale IoT deployment. *ICT Express* 5(1):1–7. <https://doi.org/10.1016/j.ict.2017.12.005>
- Popli S, Jha RK, Jain S (2019) A survey on energy efficient narrowband Internet of Things (NB-IoT): architecture, application and challenges. *IEEE Access* 7:16739–16776. <https://doi.org/10.1109/ACCESS.2018.2881533>
- Ayoub W, Samhat AE, Nouvel F, Mroue M, Prévotet J (2018) Internet of mobile things: overview of lorawan, dash7, and nb-iot in lpwans standards and supported mobility. *IEEE Commun Surv Tutor* :1–1. <https://doi.org/10.1109/COMST.2018.2877382>
- Sinha RS, Wei Y, Hwang SH (2017) A survey on LPWA technology: LoRa and NB-IoT. *ICT Express* 3(1):14–21. <https://doi.org/10.1016/j.ict.2017.03.004>
- Semtech What is LoRa?. <https://www.semtech.com/lorawhat-is-lora>. Accessed 4 November 2019
- Adhikary A, Lin X, Wang YE (2016) Performance evaluation of NB-IoT coverage. In: 2016 IEEE 84th Vehicular Technology Conference (VTC-Fall), pp 1–5. <https://doi.org/10.1109/PIMRC.2016.7794567>
- Mangalvedhe N, Ratasuk R, Ghosh A (2016) NB-IoT deployment study for low power wide area cellular IoT. In: 2016 IEEE 27th Annual International Symposium on Personal, Indoor, and Mobile Radio Communications (PIMRC), pp 1–6
- Grión FJ, Petracca GO, Lipuma DF, Amigó ER (2017) LoRa network coverage evaluation in urban and densely urban environment simulation and validation tests in autonomous city of Buenos Aires. In: 2017 XVII Workshop on Information Processing and Control (RPC), pp 1–5
- Hoeller A, Souza RD, Alves H, Alcaraz López OL, Montejó-Sánchez S, Pellenz ME (2019) Optimum lorawan configuration under wi-sun interference. *IEEE Access* 7:170936–170948. <https://doi.org/10.1109/ACCESS.2019.2955750>
- Lauridsen M, Nguyen H, Vejlgård B, Kovacs IZ, Mogensen P, Sorensen M (2017) Coverage comparison of gprs, nb-iot, lora, and sigfox in a 7800 km² area. In: 2017 IEEE 85th Vehicular Technology Conference (VTC Spring), pp 1–5
- Sigfox Sigfox, the world's leading IoT services provider. <https://www.sigfox.com/en>. Accessed 4 November 2019
- Vejlgård B, Lauridsen M, Nguyen H, Kovacs IZ, Mogensen P, Sorensen M (2017) Coverage and capacity analysis of sigfox, lora, gprs, and nb-iot. In: 2017 IEEE 85th Vehicular Technology Conference (VTC Spring), pp 1–5
- Lauridsen M, Kovacs IZ, Mogensen P, Sorensen M, Holst S (2016) Coverage and capacity analysis of lte-m and nb-iot in a rural area. In: 2016 IEEE 84th Vehicular Technology Conference (VTC-Fall), pp 1–5
- ANATEL Plano de Atribuição, Distribuição e Destinação de Radiofrequências. <http://www.anatel.gov.br/setorregulado/atribuicao-destinacao-e-distribuicao-de-faixas>. Accessed 22 November 2018
- 3GPP (2010) TR 36.814 V9.0.0; Evolved Universal Terrestrial Radio Access (E-UTRA); Further advancements for E-UTRA physical layer aspects (Release 9). Tech. rep., 3GPP. 650 Route des Lucioles - Sophia Antipolis Valbonne - France
- Frailé R, Gozálvez J, Lázaro O, Monserrat JF, Cardona N (2004) Effect of a two dimensional shadowing model on system level performance evaluation. *COST 273 TD* (04), 190
- INPE Banco de Dados Geomorfométricos do Brasil. <http://www.dsr.inpe.br/topodata/index.php>. Accessed 20 March 2018
- Semtech (2017) SX1272/73 - 860 MHz to 1020 MHz Low Power Long Range Transceiver. Rev. 3.1
- 3GPP (2015) TR45.820 - Cellular System Support for Ultra Low Complexity and Low Throughput Internet of Things. Tech. Rep., 650 Route des Lucioles - Sophia Antipolis Valbonne - France. V2.1.0
- ANATEL Relatório das Estações por localidade. <https://www.anatel.gov.br/setorregulado/telefoniamovel-outorga/lista-de-estacoes>. Accessed 2 April 2018
- Hoeller A, Souza RD, Montejó-Sánchez S, Alves H (2020) Performance analysis of single-cell adaptive data rate-enabled lorawan. *IEEE Wirel Commun Lett* :1–1. <https://doi.org/10.1109/LWC.2020.2975604>

25. Hoeller A, Souza RD, Alcaraz López OL, Alves H, de Noronha Neto M, Brante G (2018) Analysis and performance optimization of lora networks with time and antenna diversity. *IEEE Access* 6:32820–32829. <https://doi.org/10.1109/ACCESS.2018.2839064>
26. Orfanidis C, Feeney LM, Jacobsson M, Gunningberg P (2017) Investigating interference between lora and ieee 802.15.4g networks. In: 2017 IEEE 13th International Conference on Wireless and Mobile Computing, Networking and Communications (WiMob), pp 1–8
27. About LoraWAN. <https://lora-alliance.org>. Accessed 30 November 2018
28. Callebaut G, Leenders G, Buyle C, Crul S, der Perre LV (2019) LoRa physical layer evaluation for point-to-point links and coverage measurements in diverse environments. [Online]. arXiv:1909.08300
29. 3GPP - Third Generation Partnership Project Standardization of NB-IoT Completed. <http://www.3gpp.org/news-events/3gpp-news/1785-nb-iot-complete>. Accessed 4 November 2019
30. Zayas AD, Merino P (2017) The 3GPP NB-IoT system architecture for the internet of things. In: 2017 IEEE International Conference on Communications (ICC'17), pp 277–282. <https://doi.org/10.1109/ICCW.2017.7962670>
31. Ratasuk R, Vejlgard B, Mangalvedhe N, Ghosh A (2016) Nb-iot system for m2m communication. In: 2016 IEEE Wireless Communications and Networking Conference Workshops (WCNCW), pp 428–432
32. Ahmad NA, Abdul Razak NI (2019) Performance of narrow-band internet of things (nb-iot) based on repetition of downlink physical channel. In: 2019 26th International Conference on Telecommunications (ICT), pp 506–509
33. Wang YE, Lin X, Adhikary A, Grovlen A, Sui Y, Blankenship Y, Bergman J, Razaghi HS (2017) A primer on 3gpp narrow-band internet of things. *IEEE Commun Mag* 55(3):117–123. <https://doi.org/10.1109/MCOM.2017.1600510CM>
34. ETSI (2017) TS 136 101 - User Equipment (UE) radio transmission and reception. V14.3.0
35. Commscope (2013) Product specifications - cv65bsx-m. [Online]. <https://www.commscope.com/product-type/antennas/base-station-antennas-equipment/base-station-antennas/itemcv65bsx-m>
36. Mwakwata CB, Malik H, Alam MM, Moullec YL, Parand S, Mumtaz S (2019) Narrowband internet of things (nb-iot): From physical (phy) and media access control (mac) layers perspectives. *Sensors* 19(11), <https://doi.org/10.3390/s19112613>
37. Goldsmith A (2005) *Wireless communications*. Cambridge University Press, Cambridge
38. LoRa Alliance (2018) LoRaWAN 1.1 Regional Parameters. Revision: B

Publisher's note Springer Nature remains neutral with regard to jurisdictional claims in published maps and institutional affiliations.